A Certifiably Globally Optimal Solution
to the Non-Minimal Relative Pose Problem

Jesus Briales
MAPIR-UMA Group
University of Malaga, Spain
jesusbriales@uma.es

Laurent Kneip
Mobile Perception Lab
SIST ShanghaiTech
lkneip@shanghaitech.edu.cn

Javier Gonzalez-Jimenez
MAPIR-UMA Group
University of Malaga, Spain
javiergonzalez@uma.es

Abstract

Finding the relative pose between two calibrated views ranks among the most fundamental geometric vision problems. It therefore appears as somewhat a surprise that a globally optimal solver that minimizes a properly defined energy over non-minimal correspondence sets and in the original space of relative transformations has yet to be discovered. This, notably, is the contribution of the present paper. We formulate the problem as a Quadratically Constrained Quadratic Program (QCQP), which can be converted into a Semidefinite Program (SDP) using Shor's convex relaxation. While a theoretical proof for the tightness of this relaxation remains open, we prove through exhaustive validation on both simulated and real experiments that our approach always finds and certifies (a-posteriori) the global optimum of the cost function.

1. Introduction

Relative pose estimation from corresponding point pairs between two calibrated views constitutes a fundamental geometric building block in most sparse structure-from-motion and visual SLAM algorithms. In structure from motion, it helps to initialize both topology and initial values of the view-graph, which will then be used in transformation averaging schemes [15] as well as bundle adjustment [42] to obtain the joint solution over all poses and points. More specifically, using an image matching technique [29], we establish a hypothetical covisibility graph between neighbouring pairs of views, which are then verified geometrically using robust relative pose computation. In visual SLAM [26], the algorithm is used to bootstrap the computation and thus solve the chicken-and-egg problem behind the mutually depending tracking and mapping modules.

The relative pose problem is constrained by the epipolar geometry [17]. The correspondence condition between two views can notably be translated into a linear constraint by employing the well-known essential matrix. Due to scale invariance, the essential matrix has only five degrees of freedom. Five point correspondences are hence enough to constrain the relative pose [23]. The solution to the linear problem given by stacking five correspondence conditions first results in a four-dimensional nullspace. The true solution can then be recovered by applying the additional non-linear constraints that exist on the coefficients of a proper essential matrix. It can be solved using polynomial elimination techniques [28], or—more generally—the Groebner basis method [38].

The above solution is the so-called minimal solution to the problem as—ignoring special cases like degenerate 3D point configurations or zero parallax—it always leads to an exact solution for the considered correspondences (up to numerical inaccuracies). The minimal solver can be used within Ransac in order to gain robustness against outlier correspondences. An important observation in this regard is that—depending on the noise inside the data—using only five points for each hypothesis instantiation may not necessarily lead to a minimum number of Ransac iterations, as those hypotheses may be hard to bring in agreement with other points. For moderate effective outlier ratios, increased noise in the data means that sampling more points will lead to noise-cancellation effects and thus quicker convergence and better identified inlier ratios [21]. In short, a complete theory of epipolar geometry requires a non-minimal solver to the relative pose problem.

What comes as a surprise is that, despite the maturity of the field and the age of the problem, a good non-minimal solver for the calibrated relative pose problem has never been discovered. This stands in harsh contrast with the absolute pose problem, where recent solvers even achieve global and geometric optimality in closed form for an arbitrary number of 2D-to-3D correspondences [20]. The expert reader may ask why we can not use the 7 or 8-point algorithm [24, 13] to solve this problem. The reason is again explained by the noise in the data. Noise notably causes the rank-defficiency of our essential matrix constraints to

vanish. The solution is henceforth found in a smaller-dimensional nullspace. However, what we are in fact doing here is hoping that the additional non-linear constraints on our essential matrix are implicitly enforced by the noisy data. To give a more concrete example, when solving the calibrated relative pose problem with the 8-point algorithm, we are in fact solving for a fundamental matrix. We just hope that our data is strong enough to implicitly enforce the solution to also be a proper essential matrix. This, of course, is only true in the noise-free case.

It is much better to find the solution to the non-minimal problem by directly minimizing an energy defined in the 5-dimensional space of scale invariant relative poses. This is an inherently difficult problem, and an elegant globally optimal solution remains an open problem. The present paper draws inspiration from [21] who presented a cost function for the relative pose problem that is parametrized in the space of relative rotations, and can be constructed for an arbitrary number of correspondences. However, while [21] failed to solve this problem with optimality guarantees, the present paper leverages convex optimization theory to—for the first time—come up with a fast[1] probably globally optimal solution to this problem, whose optimality gets certified *a-posteriori*.

We warn the reader, this paper does not deal with outlier observations. However, we observe that even without outliers this problem is challenging enough to make traditional solvers fail in certain scenarios.

2. Further related work on global optimization

In general, finding a guaranteed globally optimal solution for non-convex optimization problems is a hard task, most often computationally intensive [14].

One natural approach consists of characterizing the globally optimal solution as one of the stationary points in the energy functional. This can be cast as a polynomial problem and solved with similar techniques than minimal problems. However, for general non-minimal problems, the number of stationary points and the size of the polynomial elimination template may explode as the order of the equations increases, often rendering the application of this procedure infeasible.

Another powerful and generic tool for NP-hard optimization problems is Branch and Bound (BnB). This proceeds by cleverly exploring (*branching*) the whole optimization space while exploiting some relaxations on the problem to skip certain regions (*bounding*). Whereas this approach has been successfully used in various geometric computer vision problems [31, 18, 21, 46], its exploratory nature often leads to slow performance (exponential time in worst-case scenario).

---

[1] At least faster than other globally optimal alternatives with guarantees such as Branch-and-Bound for the non-convex problem.

For the rest of this document we will focus instead on relaxation techniques that consider approximate, simpler versions of the optimization problem whose global optimum is easier to reach. This general idea does not necessarily lead us to the original, optimal solution. In fact, an inferior relaxation may not provide any useful information at all. On the opposite side, a *tight* relaxation is one that features the same optimal objective as the original optimization problem. A tight relaxation may provide us with the necessary information to recover the optimal solution to the original problem. If a relaxation that is tight is also convex by construction, this provides us with an appealing way to solve the original hard problem globally, as solving a convex problem globally is a much more tractable problem (typically of polynomial complexity).

Finding a good relaxation for a certain problem is not an exact science. Even though various recurrent tools exist, such as relaxing non-convex constraints to its convex hull [36, 34, 19] or applying Lagrangian duality [5], there remains much engineering involved in the combination of these tools to come up with a good relaxation.

In this work we leverage two fundamental ideas as guiding design principles: Firstly, many polynomial optimization problem can be reformulated as a Quadratically Constrained Quadratic Program (QCQP), which in turn may be relaxed onto a Semidefinite Program (SDP) via Shor's relaxation [5, 11]. This observation alone has allowed for great progress in global optimization for some problems whose SDP relaxation turns out to be tight, *e.g.* Rotation Synchronization [4, 3] or Pose Synchronization [10, 9, 6, 33, 8]. Secondly, relaxations can be *strengthened* (improved) by introducing redundant constraints [27, Chap. 13]. This trick has found applicability in the optimization literature [32, 35], *e.g.* in QCQP problems involving orthonormal constraints [1]. Briales and Gonzalez-Jimenez show in [7] that properly applying this trick is highly beneficial when working with rotation constraints in the context of the Absolute Pose problem.

3. Preliminaries

In this work we will follow similar notation and assumptions to those used by Kneip and Lynen in [21]. Specifically, we consider the central calibrated relative pose case, where each image feature can be translated into a unique unit bearing vector. Pair-wise correspondences thus consist of pairs of bearing vectors $(\boldsymbol{f}_i, \boldsymbol{f}'_i)$ pointing to the same 3D world point $\boldsymbol{p}_i$ from the first and second camera centers.

The variables of interest in the problem are the translation $\boldsymbol{t}$ and relative orientation $\boldsymbol{R}$ of the second camera frame w.r.t. that of the first camera. All the variables involved are illustrated in Fig. 1. The normalized direction $\boldsymbol{t}$ will be identified with points in the 2-sphere S^2. The 3D rotation will be featured as 3×3 orthogonal matrix with posi-
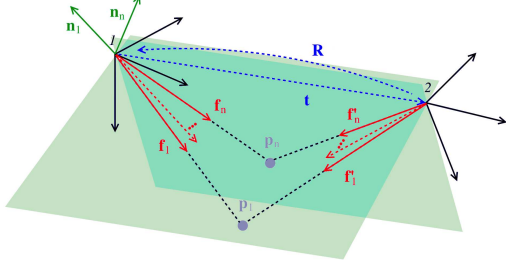
Figure 1. The relative pose problem. The measurements are given by correspondence pairs of unit bearing vectors $\{\mathbf{f}_i, \mathbf{f}'_i\}$, and the unknown variables are given by the relative orientation $\mathbf{R}$ and the direction of the relative translation $\mathbf{t}$.

tive determinant belonging to the Special Orthogonal group SO(3). Symmetric $n \times n$ matrices are denoted by Sym_n, the subindex $+$ standing for positive semidefiniteness.

Lastly, for convenience we will often refer to the list of elements in a matrix as a vector (lowercase) stacking the columns into a vector, *e.g.* $\mathbf{r} = \text{vec}(\mathbf{R})$ or $\mathbf{x} = \text{vec}(\mathbf{X})$.

4. An eigenvalue based formulation

Given the bearing vectors $\mathbf{f}_i$ and $\mathbf{f}'_i$ corresponding to each feature i in the two (calibrated) camera projections, Kneip and Lynen proposed in [21] to address the relative pose problem by enforcing the coplanarity of the moment vectors $\mathbf{m}_i = \mathbf{f}_i \times \mathbf{R}\mathbf{f}'_i$ for all the epipolar planes. This would lead to a decoupled formulation where the optimal rotation is recovered from

$$\mathbf{R}^\star = \underset{\mathbf{R} \in \text{SO}(3)}{\arg\min} \, \lambda_{\min}(\mathbf{M}(\mathbf{R})), \qquad (1)$$

with $\mathbf{M}(\mathbf{R}) = \sum_{i=1}^{N} \mathbf{m}_i \mathbf{m}_i^\top$ standing for the covariance matrix of all (in general non-unitary) epipolar plane normals. The translation direction is recovered as the eigenvector corresponding to the smallest eigenvalue of $\mathbf{M}(\mathbf{R}^\star)$:

$$\mathbf{t}^\star = \underset{\mathbf{t} \in \text{S}^2}{\arg\min} \, \mathbf{t}^\top (\mathbf{M}(\mathbf{R}^\star))\mathbf{t}. \qquad (2)$$

Whereas this decoupled approach may be compact and appealing, dealing with the non-linearity and non-convexity of the rotation suproblem (1) is far from trivial.

In this work, we take a different approach and consider instead the equivalent joint optimization problem

$$f^\star = \underset{\mathbf{R},\mathbf{t}}{\min} \, \mathbf{t}^\top \mathbf{M}(\mathbf{R})\mathbf{t}, \quad \text{s.t. } \mathbf{R} \in \text{SO}(3), \mathbf{t} \in \text{S}^2. \qquad (3)$$

The elements of the covariance matrix of normals $\mathbf{M}(\mathbf{R}) = \left[m_{ij}(\mathbf{R}) \right]_{i,j=1}^{3}$ are quadratic on the elements of the rotation matrix $\mathbf{r} = \text{vec}(\mathbf{R})$ [21]. This allows us to rewrite each component of $\mathbf{M}(\mathbf{R})$ as a quadratic function $m_{ij}(\mathbf{R}) = \mathbf{r}^\top \mathbf{C}_{ij} \mathbf{r}^\top$ with $\mathbf{C}_{ij} \in \text{Sym}_{9,+}$ a data matrix that depends

only on the problem data (see *supplementary material* for details). Using this characterization, the objective to optimize in (3) may be written as

$$f(\mathbf{R},\mathbf{t}) = \mathbf{t}^\top \mathbf{M}(\mathbf{R})\mathbf{t} = \sum_{i,j=1}^{n} t_i(\mathbf{r}^\top \mathbf{C}_{ij}\mathbf{r})t_j, \qquad (4)$$

which is a quartic function of the unknowns $(\mathbf{R}, \mathbf{t})$.

A fundamental step towards our solution is the reformulation of this quartic objective into a quadratic one by introducing the convenient auxiliary variable

$$\mathbf{X} = \mathbf{r}\mathbf{t}^\top = \left[t_1\mathbf{r} \mid t_2\mathbf{r} \mid t_3\mathbf{r} \right] = \left[r_i t_j \right]_{\substack{i=1,..,9 \\ j=1,2,3}} \qquad (5)$$

and its vectorized form

$$\mathbf{x} = \text{vec}(\mathbf{X}) = \text{vec}(\mathbf{r}\mathbf{t}^\top). \qquad (6)$$

With this definition of $\mathbf{X}$ in mind, the optimization objective (4) may be equivalently written in terms of $\mathbf{x}$, and becomes

$$f(\mathbf{R},\mathbf{t}) = \sum_{i,j=1}^{n} (t_i\mathbf{r})^\top \mathbf{C}_{ij}(t_j\mathbf{r}) = \mathbf{x}^\top \mathbf{C}\mathbf{x}, \qquad (7)$$

where the data matrix $\mathbf{C} \in \text{Sym}_{27}$ gathers all the data (matrices $\mathbf{C}_{ij}$) in the problem (3). Interested readers are invited to check the *supplementary material* for further details. With this reformulation in mind, the joint optimization problem (3) can be rewritten as

$$f^\star = \underset{\substack{\mathbf{R} \in \text{SO}(3) \\ \mathbf{t} \in \text{S}^2, \mathbf{X}}}{\min} \, \mathbf{x}^\top \mathbf{C}\mathbf{x}, \quad \text{s.t. } \mathbf{X} = \mathbf{r}\mathbf{v}^\top, \qquad (8)$$

where we assume the already presented notations for vectorized counterparts.

So far we have just rewritten the original problem in different forms, all of which are equivalent and inherently hard to solve. In particular, the last proposed formulation (8) can be seen as a Quadratically Constrained Quadratic Program (QCQP): The objective $f(\mathbf{X})$ is quadratic; the unitary constraint on the translation direction, $\mathcal{C}_t \equiv \{\mathbf{t}^\top \mathbf{t} = 1\}$, is also quadratic; a rotation matrix $\mathbf{R}$ can be fully defined solely by a set of quadratic constraints $\mathcal{C}_R$ [22, 43, 7]; and, lastly, the auxiliary constraint $\mathcal{C}_X$ on $\mathbf{X}$ (5) is also quadratic. The corresponding QCQP may be represented then as

$$\underset{\mathbf{X},\mathbf{R},\mathbf{t}}{\min} \, \mathbf{x}^\top \mathbf{C}\mathbf{x}, \quad \text{s.t. } \{\mathcal{C}_R, \mathcal{C}_t, \mathcal{C}_X\}(\mathbf{X}, \mathbf{R}, \mathbf{t}). \qquad (9)$$

Having formulated the problem as a QCQP does not make it any easier to solve. In fact, a QCQP is a very general kind of problem that comprises many NP-hard problems. However, the interest in reaching this particular formulation lies in the existence of a well-known Semidefinite Program (SDP) relaxation for QCQPs.

Next section will provide a thorough overview of a SDP relaxation for problem (8) that, as far as we empirically observed, is always tight and allows us to recover and certify the globally optimal solution $(\boldsymbol{R}^\star, \boldsymbol{t}^\star)$. An overview of the complete algorithmic approach is given in Alg. 1.

5. Global resolution through SDP relaxation

Any Quadratically Constrained Quadratic Programming (QCQP) problem instance, and in particular the introduced relative pose problem (9), may be written in the following generic form[2].

Problem QCQP (General).

$$\min_{\tilde{\boldsymbol{z}}} = \tilde{\boldsymbol{z}}^\top \tilde{\boldsymbol{Q}}_0 \tilde{\boldsymbol{z}}, \quad \tilde{\boldsymbol{z}} = \begin{bmatrix} \boldsymbol{z}^\top, 1 \end{bmatrix}^\top, \tag{10}$$

$$s.t. \ \tilde{\boldsymbol{z}}^\top \tilde{\boldsymbol{Q}}_i \tilde{\boldsymbol{z}} = 0, \quad i = 1, \ldots, m, \tag{11}$$

where $\boldsymbol{z}$ is a vector stacking all unknowns involved in the problem and $\tilde{\boldsymbol{z}}$ its homogeneization.

Note we *homogeneize* the variables and data matrices, which is a common trick to get more compact quadratic expressions [43, 7]. In our problem, $\boldsymbol{z}$ stacks the elements of our unknowns $(\boldsymbol{R}, \boldsymbol{t}, \boldsymbol{X})$. For further details on homogeneization as well as the matrices $\tilde{\boldsymbol{Q}}_i$ corresponding to the QCQP formulation of the relative pose problem we refer the interested reader to the *supplementary material*.

As previously stated, the problem (QCQP) is in general an NP-hard problem. However, it is well-known that this kind of problems can be relaxed to a convex Semidefinite Program (SDP), also known as Shor's relaxation [37, 11]. It is tightly connected to Lagrangian duality [44, 5]. The primal version of the SDP relaxation for the problem (QCQP) reads:

Problem SDP (Primal SDP).

$$d^\star = f^\star_{SDP} = \min_{\tilde{\boldsymbol{Z}}} \ \mathrm{tr}(\tilde{\boldsymbol{Q}}_0 \tilde{\boldsymbol{Z}}) \tag{12}$$

$$s.t. \ \mathrm{tr}(\tilde{\boldsymbol{Q}}_i \tilde{\boldsymbol{Z}}) = 0, \quad i = 1, \ldots, K, \tag{13}$$

$$\tilde{\boldsymbol{Z}}_{yy} = 1, \ \tilde{\boldsymbol{Z}} \succcurlyeq \boldsymbol{0}, \tag{14}$$

where $\tilde{\boldsymbol{Z}}$ is the lifted unknown matrix and the y-subindex refers to the homogeneous component in the matrix.

As a relaxation, the problem above fulfills[3]

$$d^\star = f^\star_{\mathrm{SDP}} \leq f^\star. \tag{15}$$

Our interest in this relaxation resides in the well-known fact [44] that if the relaxation (SDP) is *tight* ($d^\star = f^\star_{\mathrm{SDP}} = f^\star$)

---

[2]Note that QCQPs can in general also feature inequality constraints.

[3]We borrow the notation $d^\star$ for the optimal relaxation objective, more common for the dual of (SDP). In our context the SDP problem fulfills Slater's condition so we can safely state $d^\star = f^\star_{\mathrm{SDP}}$.

and the original problem (QCQP) features a unique global minimum, we can easily obtain the guaranteed optimal solution $\tilde{\boldsymbol{z}}^\star$ to the original problem from the optimal solution $\tilde{\boldsymbol{Z}}^\star$ to the SDP relaxation. Thus, if we are able to ensure (either theoretically or empirically) that the SDP relaxation for a given QCQP problem is tight in some scenario, this provides a highly appealing way to approach the global resolution of the original hard QCQP problem.

Unfortunately, the SDP relaxation arising from the QCQP problem corresponding to the proposed formulation (8) for the relative pose problem is in general not tight, so we may not benefit of the corresponding SDP relaxation as it is. Thus, our next goal will be to explore how we may attain this desired tight behavior in the context of the relative pose problem at hand.

5.1. Making SDP tight: Redundant constraints

In this section we are going to investigate the application of a well-known trick to our problem to improve the quality of the relaxation: The introduction of additional redundant constraints.

There are some interesting examples in the literature [45, 7] on how introducing additional redundant constraints into a QCQP problem may significantly improve the subsequent SDP relaxation (in terms of tightness). In particular, Briales and Gonzalez-Jimenez show in [7] that for a QCQP problem affected solely by a (non-convex) 3D rotation constraint, it is possible to produce an SDP relaxation that remains (empirically) tight at all times by cleverly exploiting complementary descriptions of the rotation constraints. Since our problem also features a 3D rotation constraint $\boldsymbol{R} \in \mathrm{SO}(3)$, it makes sense to apply this trick here as well.

5.1.1 Redundant rotation constraints

Briales and Gonzalez-Jimenez argue in [7] that the full family of *independent* rotation constraints for $\boldsymbol{R} \in \mathrm{SO}(3)$ that may be written as quadratic expressions is given by

$$\mathcal{C}_{\boldsymbol{R}} \equiv \begin{cases} \boldsymbol{R}^\top \boldsymbol{R} = \boldsymbol{I}_3, \quad \boldsymbol{R}\boldsymbol{R}^\top = \boldsymbol{I}_3, \\ (\boldsymbol{R}\boldsymbol{e}_i) \times (\boldsymbol{R}\boldsymbol{e}_j) = (\boldsymbol{R}\boldsymbol{e}_k), \\ \quad \forall (i,j,k) = \{(1,2,3),(2,3,1),(3,1,2)\}. \end{cases} \tag{16}$$

The set $\mathcal{C}_{\boldsymbol{R}}$ amounts to 20 independent quadratic constraints, which may be written in the form $\tilde{\boldsymbol{r}}^\top \tilde{\boldsymbol{Q}}_i \tilde{\boldsymbol{r}} = 0$.

Unfortunately, whereas in the case explored in [7] the simple introduction of these additional constraints into the problem (QCQP) would suffice to turn the corresponding relaxation (SDP) tight in practice, we found out that this is not yet enough in the present problem.

5.1.2 More redundant quadratic constraints

A convenient trick to obtain additional redundant constraints in the context of our relative pose problem (8) is to produce higher order versions of the existing constraints ($\boldsymbol{R} \in \mathrm{SO}(3), \boldsymbol{t} \in \mathrm{S}^2$) that may be still rewritten as quadratic exploiting the available auxiliary variable $\boldsymbol{X}$ (5).

Lifted sphere constraints: $\hat{\mathcal{C}}_{\boldsymbol{t}}$ We saw the translation features a single quadratic constraint $\boldsymbol{t}^\top \boldsymbol{t} = 1$. We may build redundant constraints by multiplying this constraint by r_i for $i = 1, \ldots, 9$. Even though this new constraint is implicitly cubic, we may refactor products of the form $r_i t_j$ via the auxiliary variable $\boldsymbol{X} = [r_i t_j]_{\substack{i=1,\ldots,9 \\ j=1,2,3}}$, which features all second-order combinations of this kind. As a result we obtain 9 new constraints which are implicitly cubic but expressed as quadratic constraints again.

From here on, most new constraints are built in a similar way. We multiply the quadratic constraint $\boldsymbol{t}^\top \boldsymbol{t} = 1$ by the quadratic factor $r_i r_j$ for $i, j = 1, \ldots, 9$. This time, it results in an implicitly *quartic* constraint that may be rewritten though via the auxiliary mapping $X_{ij} = r_i t_j$ into a quadratic constraint again. In this case, due to symmetry, we introduce $\binom{9}{2} = 45$ additional redundant constraints.

Lifted rotation constraints: $\hat{\mathcal{C}}_{\boldsymbol{R}}$ The case for rotation constraints is pretty much analogue to that of the sphere constraint. For *any* of the quadratic constraints previously considered for the rotation set, we may multiply this constraint by t_i for $i = 1, 2, 3$, and again rewrite pairs of the form $r_i t_j$ as X_{ij} to obtain a quadratic expression that is implicitly cubic. Similarly, if we multiply in the quadratic term $t_i t_j$ for $i, j = 1, 2, 3$ and rewrite in terms of X_{ij} where possible, we will be featuring quartic constraints written in quadratic form.

If there are 20 independent constraints in the rotation constraint set, the cubic lift produces 3 new constraints for each one, while the quartic lift results in $\binom{3}{2} = 6$ additional redundant constraints per rotation constraint. Overall, this results in $20 \cdot 9 = 180$ additional quadratic constraints.

Additional constraints on auxiliary variable: $\hat{\mathcal{C}}_{\boldsymbol{X}}$ For the auxiliary variable $\boldsymbol{X}$ it is also possible to feature additional independent constraints. In this case, it is not through a lifting procedure but simply by observing that, through its definition in (5), $\mathrm{rank}(\boldsymbol{X}) = 1$. While the rank constraint is a complex one that we do not want to directly employ here, it features though a wide set of quadratic constraints as any 2×2 minor inside the matrix $\boldsymbol{X}$ needs to be zero (otherwise $\mathrm{rank}(\boldsymbol{X}) > 1$, which contradicts its definition).

These constraints are of the form

$$X_{ab}X_{ij} - X_{ib}X_{aj} = 0, \qquad (17)$$
$$a = 1, \ldots, 9; b = 1, 2, 3; \qquad (18)$$
$$a < i \leq 9; b < j \leq 3, \qquad (19)$$

which finally results in 108 additional linearly independent constraints that depend solely on $\boldsymbol{X}$.

Surprisingly, after including this whole redundant set of underlying quadratic constraints, the SDP relaxation for the corresponding enriched QCQP problem turns out to be empirically tight in all tested circumstances, and we are ready to proceed further in our way towards the global resolution of the original problem.

5.2. Solving from the tight SDP solution: Recovery

Now that we have featured a QCQP formulation for the relative pose problem (8) whose convex SDP relaxation is empirically tight, we should be ready to proceed and solve the problem (QCQP) with global optimality guarantees.

However, we still encounter another difficulty: It is a classical result related to Shor's relaxation that if there is a unique global solution in the problem (QCQP), the tight SDP solution $\tilde{\boldsymbol{Z}}^\star$ fulfills $\mathrm{rank}(\tilde{\boldsymbol{Z}}^\star) = 1$ and we may recover $\tilde{\boldsymbol{z}}^\star$ from the low-rank decomposition $\tilde{\boldsymbol{Z}}^\star = \tilde{\boldsymbol{z}}^\star(\tilde{\boldsymbol{z}}^\star)^\top$ [44, 25]. As we show next, the condition that the original problem has a unique global minimum is not fulfilled here though. Nevertheless, we will show how we can adapt the classical low-rank decomposition trick [25] and still obtain the solution to the original problem (8) from a solution $\tilde{\boldsymbol{Z}}^\star$ to the relaxation (SDP).

5.2.1 The relative pose problem has 4 solutions

An important characteristic of original formulation (3) of the relative pose problem is that there exist symmetries in the objective. In particular,

$$f(\boldsymbol{R}, -\boldsymbol{t}) = f(\boldsymbol{R}, \boldsymbol{t}), \quad f(\boldsymbol{P}_{\boldsymbol{t}}\boldsymbol{R}, \boldsymbol{t}) = f(\boldsymbol{R}, \boldsymbol{t}), \quad (20)$$

where $\boldsymbol{P}_{\boldsymbol{t}} = 2\boldsymbol{t}\boldsymbol{t}^\top - \boldsymbol{I}_3$ is the reflection matrix w.r.t. the axis of direction $\boldsymbol{t}$. These symmetries are illustrated and proven in the *supplementary material*.

The symmetries are also consistent with the well-known fact that the estimation of the relative pose from the essential matrix also leads to 4 different solutions [24]. Indeed, our algebraic error is *exactly equivalent* to that minimized by classical solvers, *e.g.* the 8-point algorithm by Longuet-Higgins [24, 16].

As a consequence of the equivalences above, even in the well constrained, non-minimal situation, there exist 4 globally optimal solutions to the formulated problem (3):

$$\{(\boldsymbol{R}^\star, \boldsymbol{t}^\star), (\boldsymbol{R}^\star, -\boldsymbol{t}^\star), (\boldsymbol{P}_{\boldsymbol{t}^\star}\boldsymbol{R}^\star, \boldsymbol{t}^\star), (\boldsymbol{P}_{\boldsymbol{t}^\star}\boldsymbol{R}^\star, -\boldsymbol{t}^\star)\}. \quad (21)$$

Of these solutions, only one is physically realizable as the rest lead to geometries where the reconstructed 3D points lie *behind* the cameras rather than *in front of* them [24].

5.2.2 The tight primal SDP solution has rank-4

Still under the assumption that the SDP relaxation is tight, a feasible (and optimal) rank-1 solution $\tilde{\boldsymbol{Z}}_k^\star$ for the problem (SDP) can be built from any of the 4 solutions (21) to our original problem (8):

$$(\boldsymbol{R}_k^\star, \boldsymbol{t}_k^\star) \rightarrow \tilde{\boldsymbol{z}}_k^\star = \text{stack}(\boldsymbol{x}^\star, \boldsymbol{r}^\star, \boldsymbol{t}^\star, 1) \qquad (22)$$

$$\rightarrow \tilde{\boldsymbol{Z}}_k^\star = \tilde{\boldsymbol{z}}_k^\star (\tilde{\boldsymbol{z}}_k^\star)^\top. \qquad (23)$$

All of these *lifted* solutions are globally optimal as they fulfill $\text{tr}(\tilde{\boldsymbol{Q}}_0 \tilde{\boldsymbol{Z}}_k^\star) = f^\star = d^\star$ (with our tightness assumption).

By linearity of the SDP objective (12), it is easy to prove (see *supplementary material*) that any convex combination

$$\tilde{\boldsymbol{Z}}^\star = \sum_{k=1}^{4} a_k \tilde{\boldsymbol{Z}}_k^\star = \sum_{k=1}^{4} a_k \tilde{\boldsymbol{z}}_k^\star (\tilde{\boldsymbol{z}}_k^\star)^\top \qquad (24)$$

of the rank-1 solutions $\tilde{\boldsymbol{Z}}_k^\star$, with $a_k \geq 0$ and $\sum_{k=1}^{4} a_k = 1$, is also an optimal solution to the problem (SDP). The non-negativity of a_k is required to fulfill the Positive Semidefinite constraint (14) on $\tilde{\boldsymbol{Z}}$. These coefficients $\boldsymbol{a}$ may be regarded as barycentric coordinates that parameterize the set of all possible optimal solutions for problem (SDP).

In conclusion, the existence of 4 globally optimal solutions in the original problem results in the existence of infinitely many rank-4 solutions to the SDP relaxation (SDP). These solutions coincide with the convex hull of the rank-1 lifted versions of the solutions to the problem (QCQP).

5.2.3 Practical recovery of original solution

At this point, we have fully characterized the optimal solutions of the original problem (3) as well as their connection to the infinitely many solutions of the relaxation (SDP) when this is tight. In practice, we will solve the relaxation (SDP) with some off-the-shelf Primal-Dual Interior Point Method (IPM) solver (*e.g.* SeDuMi [40] or SDPT3 [41]). But these IPM approaches return *one* optimal solution $\tilde{\boldsymbol{Z}}_0^\star$ of the infinitely many available ones in the convex set $\tilde{\boldsymbol{Z}}^\star$. Now, the question of main practical interest is: Given a particular optimal solution $\tilde{\boldsymbol{Z}}_0^\star$ to the SDP problem (SDP), are we able to recover the optimal solution $(\boldsymbol{R}^\star, \boldsymbol{t}^\star)$ (and corresponding symmetries) to the original problem (3)? The answer to this question is *yes*.

In practice, a fundamental observation is that the solution provided by an IPM solver always fulfilled $\text{rank}(\tilde{\boldsymbol{Z}}_0^\star) = 4$, with an eigenvalue decomposition of the form

$$\tilde{\boldsymbol{Z}}_0^\star = \lambda_1 \boldsymbol{U}_1 \boldsymbol{U}_1^\top + \lambda_2 \boldsymbol{U}_2 \boldsymbol{U}_2^\top, \quad \boldsymbol{U}_k^\top \boldsymbol{U}_k = \boldsymbol{I}_2, \qquad (25)$$

that is, there exist two numerically distinct eigenvalues λ_1, λ_2 with multiplicity 2. From (24) we know both $\boldsymbol{U}_1$ and $\boldsymbol{U}_2$ together must span the same range space as all the global solutions to the (QCQP). In fact, another important (still empirical) observation is that each pair of eigenvectors $\boldsymbol{U}_k$ span the same range as the solutions with common rotation value:

$$\text{span}(\boldsymbol{U}_1) = \text{span}([\tilde{\boldsymbol{z}}_1^\star, \tilde{\boldsymbol{z}}_2^\star]) \leftarrow \{(\boldsymbol{R}^\star, \boldsymbol{t}^\star), (\boldsymbol{R}^\star, -\boldsymbol{t}^\star)\},$$

$$\text{span}(\boldsymbol{U}_2) = \text{span}([\tilde{\boldsymbol{z}}_3^\star, \tilde{\boldsymbol{z}}_4^\star]) \leftarrow \{(\boldsymbol{P}_{\boldsymbol{t}^\star} \boldsymbol{R}^\star, \boldsymbol{t}^\star), (\boldsymbol{P}_{\boldsymbol{t}^\star} \boldsymbol{R}^\star, -\boldsymbol{t}^\star)\}.$$

This relation allows us to recover the optimal solutions from the range space of the appropriate sub-blocks in the computed eigenvectors: Considering the case of $\boldsymbol{U}_1$, since[4] $\tilde{\boldsymbol{z}}_1^\star(\boldsymbol{r}, :) = \tilde{\boldsymbol{z}}_2^\star(\boldsymbol{r}, :) = \boldsymbol{r}^\star$ and $\tilde{\boldsymbol{z}}_1^\star(\boldsymbol{t}, :) = \tilde{\boldsymbol{z}}_2^\star(\boldsymbol{t}, :) = \boldsymbol{t}^\star$,

$$\text{span}(\boldsymbol{U}_1(\boldsymbol{r}, :)) = \text{span}(\boldsymbol{r}^\star), \quad \text{span}(\boldsymbol{U}_1(\boldsymbol{t}, :)) = \text{span}(\boldsymbol{t}^\star).$$

As a result, if $\boldsymbol{V}_{\boldsymbol{r}} \in \mathbb{R}^9$ and $\boldsymbol{V}_{\boldsymbol{t}} \in \mathbb{R}^3$ are basis vectors for the rank-1 subspaces $\text{span}(\boldsymbol{U}_1(\boldsymbol{r}, :))$ and $\text{span}(\boldsymbol{U}_1(\boldsymbol{t}, :))$ respectively, the optimal solutions within the range of $\boldsymbol{U}_1$ can be obtained by simple normalization:

$$\text{vec}(\boldsymbol{R}^\star) = \sqrt{3} \frac{\boldsymbol{V}_{\boldsymbol{r}}}{\|\boldsymbol{V}_{\boldsymbol{r}}\|}, \quad \boldsymbol{t}^\star = \frac{\boldsymbol{V}_{\boldsymbol{t}}}{\|\boldsymbol{V}_{\boldsymbol{t}}\|}. \qquad (26)$$

Similar relations hold for the solutions contained in $\boldsymbol{U}_2$.

Further discussions on these empirical observations can be found in Section 8 of the *supplementary material*.

5.2.4 A-posteriori global optimality guarantees

Throughout the previous subsections we have extensively built upon the assumption that the relaxation (SDP) is tight. This, however, is not known a-priori for a given problem. Thus, the way we proceed in practice is as follows: First, we proceed with the described approach as if the relaxation (SDP) was indeed tight, obtaining a set of (symmetric) candidate solutions $(\hat{\boldsymbol{R}}_k, \hat{\boldsymbol{t}}_k)$. Then, we check the primal feasibility ($\hat{\boldsymbol{R}}_k \in \text{SO}(3)$, $\hat{\boldsymbol{t}}_k \in \text{S}^2$) of these candidates. If the relaxation was tight, these candidates should be indeed feasible. Just for numerical stability, we may project these candidates into their closest point in their manifold (by classical means), and check that $d^\star = f(\hat{\boldsymbol{R}}_k, \hat{\boldsymbol{t}}_k)$ as a *certificate of optimality*. If this property is fulfilled, this proves our tightness assumption and these feasible candidate points are indeed the global solutions of the original problem (3).

The complete algorithm is characterized in Alg. 1.

6. Experiments

The main goal of this section will be to empirically prove the surprising and desirable fact that the proposed SDP relaxation always turns out to be tight in practice, providing a (a-posteriori) guaranteed optimal solution.

---

[4] We use $(\boldsymbol{r}, :)$ and $(\boldsymbol{t}, :)$ as Matlab-like notation to refer to the set of indexes corresponding to $\boldsymbol{r}$ and $\boldsymbol{t}$ within $\boldsymbol{z}$ by convention (see Sec. 5).

Algorithm 1: Solving relative pose via SDP relaxation

Input: List of correspondences $\{(\boldsymbol{f}_i, \boldsymbol{f}'_i)\}_{i=1}^N$
Output: Probably certifiable global solution $(\boldsymbol{R}^\star, \boldsymbol{t}^\star)$

    `/* build (QCQP) constr. mat. (full set) */`
1   $\{\tilde{\boldsymbol{Q}}_i\}_{i=1}^K \leftarrow \{\hat{\mathcal{C}}_{\boldsymbol{R}}, \hat{\mathcal{C}}_{\boldsymbol{t}}, \hat{\mathcal{C}}_{\boldsymbol{X}}\}(\boldsymbol{X}, \boldsymbol{R}, \boldsymbol{t})$;
    `/* build (QCQP) objective data matrix */`
2   $\tilde{\boldsymbol{Q}}_0 \leftarrow \boldsymbol{C} \leftarrow \{\boldsymbol{C}_{ij}\}_{i,j=1,2,3} \leftarrow \{(\boldsymbol{f}_i, \boldsymbol{f}'_i)\}_{i=1}^N$
    `/* solve relaxation (SDP) */`
3   $(\tilde{\boldsymbol{Z}}_0^\star, d^\star) \leftarrow \text{SDP}(\tilde{\boldsymbol{Q}}_0, \{\tilde{\boldsymbol{Q}}_i\}_{i=1}^K)$;   `// IPM [41, 40]`
    `/* compute low-rank eig-decomposition */`
4   $\sum_k \lambda_k \boldsymbol{u}_k \boldsymbol{u}_k^\top \leftarrow \tilde{\boldsymbol{Z}}_0^\star, \quad \lambda_k \geq \lambda_{k+1} \ \forall k$;
5   $\text{ASSERT}((\lambda_1 = \lambda_2) \wedge (\lambda_3 = \lambda_4) \wedge (\lambda_k = 0, \ \forall k > 4))$;
    `/* recover candidate sol. (Sec. 5.2.3) */`
6   $(\hat{\boldsymbol{R}}_k, \hat{\boldsymbol{t}}_k)_{k=1,2} \leftarrow \{\boldsymbol{u}_1, \boldsymbol{u}_2\}$
7   $(\hat{\boldsymbol{R}}_k, \hat{\boldsymbol{t}}_k)_{k=3,4} \leftarrow \{\boldsymbol{u}_3, \boldsymbol{u}_4\}$
    `/* project candidates to feasible set */`
8   $\hat{\boldsymbol{R}}_k \leftarrow \text{proj}_{\text{SO}(3)}(\hat{\boldsymbol{R}}_k), \hat{\boldsymbol{t}}_k \leftarrow \text{proj}_{\text{S}^2}(\hat{\boldsymbol{t}}_k), \forall k = 1, .., 4$;
    `/* check optim. gap, certify optimality */`
9   $\Delta_k = f(\hat{\boldsymbol{R}}_k, \hat{\boldsymbol{t}}_k) - d^\star$;
10   $\text{ASSERT}(\Delta_k < \texttt{tol}, \forall k = 1, .., 4), \texttt{tol} \sim 10^{-9}$;
    `/* disambiguate realizable solution [24] */`
11   **return** $(\boldsymbol{R}^\star, \boldsymbol{t}^\star) \leftarrow \{(\hat{\boldsymbol{R}}_k, \hat{\boldsymbol{t}}_k)\}$

For this purpose, we evaluated the proposed approach, SDP, in an extensive batch of experiments that span a wide set of problem configurations, both on synthetic and real data. The problem (SDP) was modeled with CVX [12] and the IPM solver used in practice was SDPT3 [41], which takes around 1 second to solve on a common consumer-grade computer. We compared our performance to that of the state-of-the-art (local) eigensolver proposed by Kneip and Lynen [21], which we initialized using the classical 8-point algorithm by Longuet-Higgins [24]. The linear closed-form estimator is referred to as 8pt, and its refined version through the eigensolver as 8pt+eig. Note that all of these methods feature exactly the same equivalent optimization objective, so it is fair to compare all of them in terms of the attained objective value.

In the subsequent evaluation, we will rely on two different metrics. First, since the SDP relaxation (SDP) provides a lower bound $d^\star$ on the optimal objective $f^\star$, we define the optimality gap for a candidate solution $\Delta = \hat{f} - d^\star$. If this optimality gap is numerically zero, we can assert the candidate is globally optimal (check Section 5). Despite its theoretical soundness, the optimality gap measure may be little intuitive. Thus, we also provide the more intuitive *orientation error* measure of a given candidate w.r.t. a known-optimal solution[5]. For space's sake, we skip here the er-

---

[5] Since the duality gap always vanishes numerically for the solution of SDP, this will be our optimal reference.

---

ror measure on the translation direction component, which leads to similar conclusions to those from orientation error.

6.1. Synthetic data

We generate random problems by the following procedure: We fix the first camera at the origin (orientation is identity). Then, we generate a set of 3D world points randomly distributed within a bounded region of the space that lies fully inside the Field of View (FOV) of the first camera, and at least one meter away from the camera. Next, we generate a random pose for the second camera with bounded translation parallax and constrained so that the world points also lie within its FOV. This way we obtain random relative poses that are consistent with the physical constraints that would exist in practical situations. From this point, we proceed as in Kneip and Lynen [21]: bearing vectors for each 3D point are computed and corrupted with some pixel noise assuming a focal length of 800 pixels for the camera.

The synthetic world allows us to tune at will several relevant parameters of the problem: The noise level in the image features (σ, in `pix`), the number of observed features (N), the FOV of the camera (θ, in $\deg$), and the parallax magnitude ($\|\boldsymbol{t}\|$, in `m`). For the evaluation, we assumed a reference set of parameters $\sigma = 0.5\texttt{pix}$, $N = 10$, $\theta = 100 \deg$, and $\|\boldsymbol{t}\| \leq 2\texttt{m}$, and then proceed to analyze the behavior of the evaluated methods by modifying one single parameter. The results of the synthetic evaluation are collected in Fig. 2. We display the evaluation metrics both with a boxplot and a superimposed histogram of concrete values. A shallow boxplot collapsed in 0 points to a frequent global convergence, whereas outliers (when existent) clearly reveal failure cases with wrong converge. In the evaluation, we generated 200 different instances for each problem configuration.

In these results we see the proposed approach SDP always attained a zero optimality gap ($\Delta_{\text{SDP}} \sim o(10^{-10})$ in practice), whereas the optimality gap for the other methods rose up to $\Delta_{\text{8pt}}, \Delta_{\text{8pt+eig}} \sim o(10^{-3})$ in some cases. Interestingly, even though these optimality gaps do not seem too large, the analysis of the corresponding rotation error reveals this gap is actually important, as it incurs in large errors in the estimated orientation parameter. This is consistent with the fact that the squared error terms minimized in the objective are bounded by 1, and in general, even if erroneous, are not too high. This seems to result in sub-optimal local minima having objective values dangerously close to those of the global solution [21], which may lead to missing the true global solution.

A close analysis on how often the alternative solver 8pt+eig fails to converge provides valuable feedback about the inherent difficulty of the problem. The obtained results suggest that difficulty increases with high level of noise in observations and low numbers of observations,
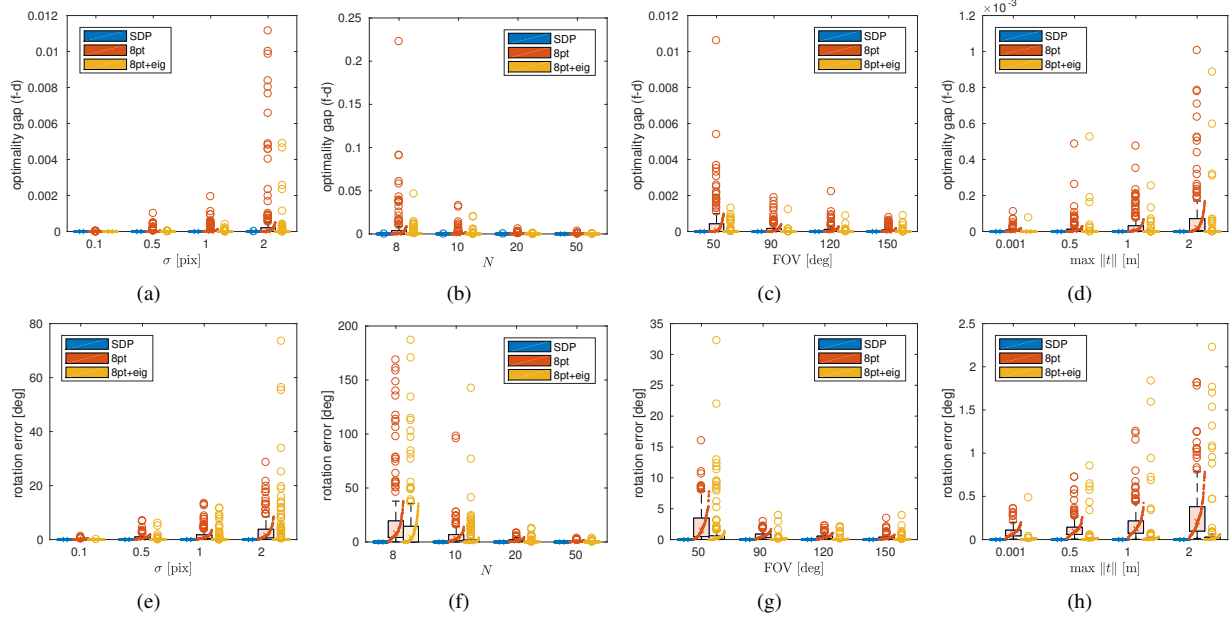
Figure 2. Optimality gap and rotation error vs. all tunable parameters. Default values: $\sigma = 0.5\texttt{pix}$, $N = 10$, FOV $= 100$ deg, and $\|\boldsymbol{t}\| \leq 2$m. Note that despite choosing $\sigma \leq 2\texttt{pix}$ for visualization, experiments were performed with virtually unbounded noise ($\sigma \sim 10^3\texttt{pix}$), still leading to tight relaxations in all cases, thus supporting the generality of tightness for this relaxation.

which is an expectable behavior [30, 7]. Also, an increasing FOV makes the problem easier, as this results in a better constraining of the optimization objective [21]. A larger parallax hindered the performance of 8pt and 8pt+eig.

We also evaluated our approach in the pure rotation scenario. Interestingly, whereas the relaxation in this case also remains tight, some additional challenges appear when recovering the optimal solutions from the SDP solution, specially in the noiseless case where the number of solutions doubles. This is an interesting case that we keep however for further analysis in future work, due to its extension.

6.2. Real data

For the evaluation on real data, we took pairs of overlapping images from the TUM benchmark sequence [39], which provides both accurate ground-truth camera poses as well as the intrinsic camera calibration. We extract and match SURF features in the images, filtering outliers by thresholding on the reprojection error of triangulated correspondences. Finally, we run the same algorithms as in the previous section. The results, which are displayed in the *supplementary material* due to space limitations, are consistent with the conclusions reached in the synthetic case. In particular, our proposed approach continued to find and certify the globally optimal solution.

The general conclusion in view of our experimental results is that the concrete configuration of a relative pose problem may have a great impact in the hardness of converging to the global solution by traditional means. Yet,

our proposed SDP relaxation-based approach always succeeded, providing the optimal solution together with a certificate of optimality based on duality theory.

7. Conclusions

This work solves a previously unsatisfyingly solved geometric problem of fundamental interest: Direct and optimal computation of the relative pose between two calibrated images over an arbitrary number of correspondences. Previous solvers either solve only for sub-optimal linearizations, or proceed by computationally less attractive exhaustive search strategies such as branch-and-bound. We have proposed a tailored (non-trivial) formulation of the problem as a Quadratically Constrained Quadratic Program for which Shor's relaxation is tight in 100% of the experimentally evaluated problems, allowing us to *recover* and *certify* the globally optimal solution.

We find these results very exciting, and we think there is still significant space for improvement, both in solving the underlying SDP relaxation with specialized solvers that exploit the low-rank structure of the problem as well as in leveraging these results in different scenarios, such as the development of computationally attractive Probably Certifiably Correct algorithms [2] for the problem at hand.

References

[1] K. Anstreicher and H. Wolkowicz. On Lagrangian relaxation of quadratic matrix constraints. *SIAM Journal on Matrix Analysis and Applications*, 22(1):41–55, 2000.

[2] A. Bandeira. A note on probably certifiably correct algorithms. *Comptes Rendus Mathematique*, 2016.

[3] A. Bandeira, N. Boumal, and A. Singer. Tightness of the maximum likelihood semidefinite relaxation for angular synchronization. *Mathematical Programming*, 2016.

[4] N. Boumal. A Riemannian low-rank method for optimization over semidefinite matrices with block-diagonal constraints. *arXiv preprint arXiv:1506.00575*, 2015.

[5] S. Boyd and L. Vandenberghe. *Convex optimization*. Cambridge University Press, 2004.

[6] J. Briales and J. González-Jiménez. Fast Global Optimality Verification in 3D SLAM. In *Proc. Int. Conf. Intell. Robots Syst. (IROS)*, Daejeon, 2016. IEEE/RSJ.

[7] J. Briales and J. González-Jiménez. Convex Global 3D Registration with Lagrangian Duality. In *International Conference on Computer Vision and Pattern Recognition*, jul 2017.

[8] J. Briales and J. González-Jiménez. Initialization of 3D Pose Graph Optimization using Lagrangian duality. In *Int. Conf. on Robotics and Automation (ICRA)*. IEEE, 2017.

[9] L. Carlone, G. C. Calafiore, C. Tommolillo, and F. Dellaert. Planar Pose Graph Optimization: Duality, Optimal Solutions, and Verification. *IEEE Transactions on Robotics*, 32(3):545–565, 2016.

[10] L. Carlone, D. M. Rosen, G. Calafiore, J. J. Leonard, and F. Dellaert. Lagrangian duality in 3D SLAM: Verification techniques and optimal solutions. In *Proc. Int. Conf. Intell. Robots Syst. (IROS)*, pages 125–132, Hamburg, sep 2015.

[11] Y. Ding. On efficient semidefinite relaxations for quadratically constrained quadratic programming. 2007.

[12] M. Grant and S. Boyd. {CVX}: Matlab Software for Disciplined Convex Programming, version 2.1. \url{http://cvxr.com/cvx}, 2014.

[13] R. Hartley. In Defense of the Eight-Point Algorithm. 19(6):580–593, 1997.

[14] R. Hartley and F. Kahl. Optimal Algorithms in Multiview Geometry. In *Computer Vision ACCV 2007*, pages 13–34. Springer Berlin Heidelberg, Berlin, Heidelberg.

[15] R. Hartley, J. Trumpf, Y. Dai, and H. Li. Rotation Averaging. *International Journal of Computer Vision*, 103(3):267–305, jan 2013.

[16] R. Hartley and A. Zisserman. *Multiple View Geometry in Computer Vision*. Cambridge University Press, New York, NY, USA, 2 edition, 2003.

[17] R. Hartley and A. Zisserman. *Multiple View Geometry in Computer Vision*. Cambridge University Press, New York, NY, USA, second edition, 2004.

[18] R. I. Hartley and F. Kahl. Global optimization through rotation space search. *International Journal of Computer Vision*, 82(1):64–79, 2009.

[19] Y. Khoo and A. Kapoor. Non-iterative rigid 2D/3D point-set registration using semidefinite programming. *IEEE Transactions on Image Processing*, 25(7):2956–2970, 2016.

[20] L. Kneip, H. Li, and Y. Seo. Upnp: An optimal o (n) solution to the absolute pose problem with universal applicability. In *Computer Vision–ECCV 2014*, pages 127–142. Springer, 2014.

[21] L. Kneip and S. Lynen. Direct optimization of frame-to-frame rotation. In *Computer Vision (ICCV), 2013 IEEE International Conference on*, pages 2352–2359. IEEE, 2013.

[22] L. Kneip, R. Siegwart, and M. Pollefeys. *Finding the exact rotation between two images independently of the translation.* Springer, 2012.

[23] E. Kruppa. Zur Ermittlung eines Objektes aus zwei Perspektiven mit innerer Orientierung. *Sitzgsber. Akad. Wien, Math. Naturw. Abt., IIa.*, 122:1939–1948, 1913.

[24] H. C. Longuet-Higgins. A computer algorithm for reconstructing a scene from two projections. *Nature*, 293(5828):133–135, 1981.

[25] Z.-Q. Luo, W.-K. Ma, A. M.-C. So, Y. Ye, and S. Zhang. Semidefinite relaxation of quadratic optimization problems. *IEEE Signal Processing Magazine*, 27(3):20–34, 2010.

[26] R. Mur-Artal, J. M. M. Montiel, and J. D. Tardós. ORB-SLAM: A Versatile and Accurate Monocular SLAM System. *IEEE Transactions on Robotics (T-RO)*, 31(5):1147–1163, 2015.

[27] Y. Nesterov, H. Wolkowicz, and Y. Ye. Semidefinite programming relaxations of nonconvex quadratic optimization. In *Handbook of semidefinite programming*, pages 361–419. Springer, 2000.

[28] D. Nistér. An efficient solution to the five-point relative pose problem. *IEEE Transactions on Pattern Analysis and Machine Intelligence (PAMI)*, 26(6):756–777, 2004.

[29] D. Nistér and H. Stewénius. Scalable recognition with a vocabulary tree. 2006.

[30] C. Olsson and A. Eriksson. Solving quadratically constrained geometrical problems using lagrangian duality. In *Pattern Recognition, 2008. ICPR 2008. 19th International Conference on*, pages 1–5. IEEE, 2008.

[31] C. Olsson, F. Kahl, and M. Oskarsson. Branch-and-Bound Methods for Euclidean Registration Problems. *IEEE Trans. Pattern Anal. Mach. Intell.*, 31(5):783–794, 2009.

[32] P. A. Parrilo and S. Lall. Semidefinite programming relaxations and algebraic optimization in control. *European Journal of Control*, 9(2):307–321, 2003.

[33] D. M. Rosen, L. Carlone, A. S. Bandeira, and J. J. Leonard. SE-Sync: A Certifiably Correct Algorithm for Synchronization over the Special Euclidean Group. *arXiv preprint arXiv:1612.07386*, pages 1–49, 2016.

[34] D. M. Rosen, C. DuHadway, and J. J. Leonard. A convex relaxation for approximate global optimization in simultaneous localization and mapping. In *Proc. Int. Conf. Robot. and Autom. (ICRA)*, pages 5822–5829, Seattle, 2015. IEEE.

[35] J. P. Ruiz and I. E. Grossmann. Using redundancy to strengthen the relaxation for the global optimization of MINLP problems. *Computers & Chemical Engineering*, 35(12):2729–2740, 2011.

[36] J. Saunderson, P. A. Parrilo, and A. S. Willsky. Semidefinite descriptions of the convex hull of rotation matrices. *arXiv preprint arXiv:1403.4914*, 2014.

[37] N. Z. Shor. Quadratic optimization problems. *Sov. J. Comput. Syst. Sci.*, 25(6):1–11, 1987.

[38] H. D. Stewénius, C. Engels, and D. Nistér. Recent developments on direct relative orientation. *ISPRS Journal of Photogrammetry and Remote Sensing*, 60(4):284–294, 2006.

[39] J. Sturm and N. Engelhard. A benchmark for the evaluation of RGB-D SLAM systems. *Intelligent Robots and Systems (IROS), 2012 IEEE/RSJ International Conference on*, 2012.

[40] J. F. Sturm. Using SeDuMi 1.02, a MATLAB toolbox for optimization over symmetric cones. *Optimization methods and software*, 11(1-4):625–653, 1999.

[41] K.-C. Toh, M. J. Todd, and R. H. Tütüncü. SDPT3a MAT-LAB software package for semidefinite programming, version 1.3. *Optim. methods Softw.*, 11(1-4):545–581, 1999.

[42] B. Triggs, P. McLauchlan, R. Hartley, and A. Fitzgibbon. Bundle adjustment - a modern synthesis. In *Proceedings of the International Workshop on Vision Algorithms: Theory and Practice (ICCV)*, pages 298–372, Corfu, Greece, 1999.

[43] R. Tron, D. M. Rosen, and L. Carlone. On the Inclusion of Determinant Constraints in Lagrangian Duality for 3D SLAM. In *Proc. Robotics: Science and Systems (RSS), Workshop The Problem of Mobile Sensors*, 2015.

[44] L. Vandenberghe and S. Boyd. Semidefinite programming. *SIAM review*, 38(1):49–95, 1996.

[45] H. Wolkowicz. A note on lack of strong duality for quadratic problems with orthogonal constraints. *European Journal of Operational Research*, 143(2):356–364, 2002.

[46] J. Yang, H. Li, and Y. Jia. Optimal essential matrix estimation via inlier-set maximisation. In *Proceedings of the European Conference on Computer Vision (ECCV)*, 2014.